Germanium-Based Detectors for Gamma-Ray Imaging and Spectroscopy[1]

M. Amman [a,*], P. N. Luke [a], S. E. Boggs [b]

[a] *Ernest Orlando Lawrence Berkeley National Laboratory, University of California, Berkeley, California 94720, USA*

[b] *Department of Physics, University of California, Berkeley, California 94720, USA*

Abstract

Germanium-based detectors are the standard technology used for gamma-ray spectroscopy when high efficiency and excellent energy resolution are desired. By dividing the electrical contacts on these detectors into segments, the locations of the gamma-ray interaction events within the detectors can be determined as well as the deposited energies. This enables simultaneous gamma-ray imaging and spectroscopy and leads to applications in the areas of astronomy, nuclear physics, environmental remediation, nuclear nonproliferation, and homeland security. Producing the fine-pitched electrode segmentation often required for imaging has been problematic in the past. To address this issue, we have developed an amorphous-semiconductor contact technology. Using this technology, fully passivated detectors with closely spaced contacts can be produced using a simple fabrication process. The current state of the amorphous-semiconductor contact technology and the challenges that remain will be given in this paper.

Suggested PACS: 07.85.Nc; 29.40.Gx; 29.40.Wk; 95.55.Ka

Keywords: gamma-ray imaging; gamma-ray spectroscopy; germanium detector; orthogonal strip; position sensing;

*Corresponding author. Tel.: + 1 510 486 5638; fax: + 1 510 486 5857; e-mail: Mark_Amman@lbl.gov.

[1] This research was supported by NASA Contract NNG04WF321 and the U.S. Department of Energy under Contract No. DE-AC02-05CH11231.

1. Introduction

There are several advantages for choosing high-purity Ge for gamma-ray spectroscopy. These include (1) commercial availability of large detector volumes (10 cm diameter boules), (2) ability to fully deplete thick detector layers (> 1 cm), (3) relatively high atomic number, (4) near perfect charge collection, and (5) favorable charge generation statistics. The first three advantages lead to high detection efficiency and the later two to excellent energy resolution (< 0.2 % FWHM at 1.33 MeV). However, because of the small bandgap energy of Ge, the detectors do require cryogenic cooling (to near 100 K) in order to reduce the thermal generation of electron-hole pairs that tend to obscure the small signal current generated by the gamma-ray interactions.

Combining gamma-ray imaging with spectroscopy forms a powerful tool for basic scientific research and practical radioisotope detection and characterization. Gamma-ray imaging often relies on detectors that can accurately determine the location of the gamma-ray interaction events within the detector volumes as well as the deposited energies [1]. The development of high spectroscopic performance Ge-based imaging instruments has been hampered in the past by difficulties in producing such position-sensitive detectors. The subject of this paper is the detector technology developed at Lawrence Berkeley National Laboratory (LBNL) that enables the simple production of Ge-based gamma-ray detectors with fine spatial resolution. In particular we describe the amorphous-semiconductor contact technology [2-9], its advantages, and the developmental work that remains to be done.

2. Amorphous-semiconductor contacts

A simple single-element Ge gamma-ray detector (see Figure 1a) consists of a block of high-purity Ge material in which n+ and p+ impurity-doped electrical contacts have been fabricated on opposite sides of the block. The detector is operated as a fully-depleted reverse-biased diode and spectroscopy is performed by measuring the electron-hole pair charge generated by each gamma-ray interaction event within the detector. The standard contact technology for such a detector consists of a Li-diffused n+ contact and a B-implanted p+ contact. Both contact types are robust, can withstand high electric fields, and lead to low charge carrier injection.

To produce a position-sensitive detector for imaging applications, the electrical contacts on the detector are divided into segments as shown in Figure 1b. This can be readily done on the B-implanted contact [10,11] but is problematic on the Li-diffused side because of the contact thickness and the continued Li diffusion into Ge at room temperature. Furthermore, the inter-contact surfaces for both contact types should be passivated to obtain long-term detector stability, thereby necessitating additional processing steps. An alternative technology capable of producing position-sensitive detectors is the amorphous semiconductor contact developed at LBNL. With this technology (see Figure 1c), the contacts are formed by first coating all surfaces of the Ge crystal with a thin film of high-resistivity amorphous semiconductor (typically Ge or Si). Metal layers in the desired pattern are then deposited on top of the amorphous layer to complete the contact fabrication. The physical contact area in such a detector is defined by this low-resistivity metallization. However, most of the important electrical properties of the contact structure are dictated by the amorphous semiconductor layer and the amorphous semiconductor to crystalline Ge interface. The advantages of this technology are (1) fabrication simplicity, (2) thin contact dead layers, (3) complete surface passivation since amorphous Ge (a-Ge) layers are commonly used for Ge passivation, (4) fine achievable contact pitches, and (5) bipolar blocking contacts. Much of the remainder of this paper will focus on describing how the contacts function and the improvements needed to make this a more widely adopted contact technology.

The amorphous semiconductor contacts on Ge behave much like Schottky metal-semiconductor contacts with electron and hole barriers to charge injection typically equal to about half the bandgap energy of Ge. Consequently, the contacts can block the injection of both types of charge carriers and the same contact can therefore operate with low leakage current under either bias polarity. This is in contrast to conventional impurity-doped contacts which block injection under only one bias polarity, and metal-Ge surface barrier contacts that typically block well only when negatively biased. The bipolar blocking behavior is demonstrated in Figure 2 where the leakage current from an a-Ge contact detector is plotted for both negative and positive detector biases. Under either detector polarity, one of the a-Ge contacts is positively biased and the other is negatively biased, yet low leakage is obtained at typical operating temperatures.

The electron or hole energy barrier to charge injection is an important property of a contact that dictates the level of charge injected into the detector which in turn can impact energy resolution if excessive. To determine the electron barrier of an amorphous contact, we fabricate a detector consisting of p-type Ge with a Li n+ contact on one side and the amorphous contact to be evaluated on the other. Under reverse bias, the depletion within this detector begins at the Li contact and, as the bias is increased, extends towards the amorphous contact. At full depletion, the field penetrates to the amorphous contact and a step increase in the leakage current is observed that is a result of electron injection at the amorphous contact. By measuring this step height as a function of temperature and fitting the data to a simple thermionic emission model [12], we are able to extract out the electron barrier. An example measurement from an n+/p-type Ge/a-Ge detector is given in Figure 3a and the barrier height extraction is shown in Figure 4 plot (a). Similarly, an n-type Ge detector with a B-implanted p+ contact (or Pd metal-semiconductor contact) on one side and the amorphous contact on the opposing side can be used to determine the hole barrier of the amorphous contact. An example measurement from a Pd/n-type Ge/a-Ge detector is shown in Figure 3b and the hole barrier height determination in Figure 4 plot (b). From simple Schottky contact theory, the sum of the electron barrier and the hole barrier for a particular contact should equal the Ge bandgap energy. From Figure 4, we see that the sum for this particular a-Ge contact is 0.68 eV and is reasonably close to the Ge bandgap energy (at the average measurement temperature of 135 K) of 0.72 eV.

The barrier heights of the amorphous-semiconductor contacts depend in part on the semiconductor used and the method by which they are deposited. This is an important tool that can be used to optimize detector performance. Our standard method to deposit the amorphous films is rf sputtering in pure Ar and Ar-H_2 gas mixtures. The addition of H_2 to the sputter gas produces a-Ge and a-Si films of substantially higher resistivities than those obtained with pure Ar sputtering and also impacts the barrier heights. A summary of the barrier heights measured for a few different types of amorphous semiconductor contacts is given in Table 1 [13]. The data show that a-Ge sputtered in pure Ar (a-Ge (Ar)) produces electron and hole barriers of nearly the same value, which is approximately half of the Ge bandgap. If, for fabrication simplicity, a single contact process was used to produce all contacts on a detector, it would seem that the a-Ge (Ar) contact would be best since it should lead to the lowest detector leakage. However, the resistivity of the a-Ge (Ar) can potentially be low enough to degrade energy resolution as a result of the Johnson noise associated with the low inter-contact resistance caused by the a-Ge (Ar) layer. The addition of H_2 to the sputter gas increases the a-Ge film resistivity by several orders of magnitude and solves this problem. In part, for this reason, we typically use a-Ge (Ar+H_2) to produce finely segmented detectors.

Detectors produced with a-Ge (Ar+17.5% H_2) contacts for both the positive and negative contacts operate with low leakage and good spectroscopic performance at temperatures near that of liquid nitrogen. If, however, the detector temperature is increased to about 90 K or above, the leakage current can be significant enough to degrade the detector energy resolution. The temperature dependence of the leakage current for an all a-Ge (Ar+17.5% H_2) contact detector is shown in Figure 5a. The leakage current step increase exhibited in the plots results from electron injection at the negative contact when full depletion is reached. As the data of Table 1 indicates, the addition of H_2 to the sputter gas has not only increased the a-Ge film resistivity, but it has also increased the hole barrier at the expense of the electron barrier. The reduced electron barrier is then the primary cause of the leakage in Figure 5a. We have demonstrated that replacing the negative contact with the higher electron barrier a-Si contact substantially lowers the detector leakage at the higher temperatures. This is shown in Figure 5b. Such a detector configuration is appropriate when higher operating temperatures are desired.

Germanium-based gamma-ray detectors with a-Ge contacts have successfully been produced for several prototype imaging instruments [4,14-17]. A typical configuration for these detectors is the orthogonal-strip geometry with strip pitches between 1 and 2 mm and detector volumes as large as 160 cm^3. Excellent energy resolution and three-dimensional position detection are achieved with these detectors. We have also demonstrated the fine-electrode segmentation capability of the contacts by fabricating strip detectors with pitches down to 50 μm.

3. Future improvements

Despite the substantial success achieved with Ge-based detectors fabricated using amorphous semiconductor contacts, issues remain to be resolved before the full potential of the devices will be realized in large-scale instruments. These issues include excessive leakage at temperatures significantly above that of liquid nitrogen, leakage current degradation with temperature cycling, and charge collection to inter-contact surfaces. The excessive leakage current issue was discussed in the previous section and, as we have shown, can be addressed through the development and optimization of the a-Ge/Ge/a-Si detector configuration and other similar structures.

Cycling the temperature of an amorphous contact Ge detector from cryogenic temperatures to room temperature and then back to a low temperature again typically causes the leakage current of the detector to increase at the operating temperature. Such temperature cycling is unavoidable in the detector evaluation and instrument assembly process. The gradual increase in the leakage caused by this cycling can ultimately lead to degraded energy resolution. We have found that the extent of this degradation is dependent on the parameters used during the sputter deposition of the amorphous semiconductor layer (temperature, power, sputter gas mixture and pressure) and can be substantially reduced or eliminated through judicious selection of the parameters.

When charge from a gamma-ray interaction event is collected to the surfaces separating adjacent contacts rather than to the contacts themselves, a deficit in the measured charge results that can degrade spectroscopic performance [5-7]. The extent of this incomplete charge collection is affected by the nature of the amorphous semiconductor layer on the inter-contact surfaces. Several possible approaches exist to lessen or eliminate this problem and include (1) optimizing the amorphous layer and surface processing so that charge accumulation inhibits the collection of signal charges at the inter-contact surface [7], (2) minimizing the area of inter-contact surfaces at the price of greater inter-contact capacitance and, consequently, electronic noise, (3) etching away the amorphous semiconductor surface layer between contacts [8], (4) making use of field-shaping electrodes [6,7], and (5) signal processing to correct for the charge loss. Further work in this area is required in order to determine the effectiveness and reliability of each approach as well as to identify any shortcomings so that the best solutions can be applied to future detectors.

References

[1] G. W. Phillips, Nucl. Instr. Meth. B 99 (1995) 674, and references therein.

[2] W. L. Hansen and E. E. Haller, IEEE Trans. Nucl. Sci. 24 (1977) 61.

[3] P. N. Luke, C. P. Cork, N. W. Madden, C. S. Rossington, et al., IEEE Trans. Nucl. Sci. 39 (1992) 590.

[4] P. N. Luke, R. H. Pehl, and F. A. Dilmanian, IEEE Trans. Nucl. Sci. 41 (1994) 976.

[5] P. N. Luke, M. Amman, B. F. Phlips, W. N. Johnson, et al., IEEE Trans. Nucl. Sci. 47 (2000) 1360.

[6] M. Amman and P. N. Luke, Nucl. Instr. Meth. A 452 (2000) 155.

[7] M. Amman and P. N. Luke, Proceedings of the SPIE 4141 (2000) 144.

[8] D. Protic and T. Krings, IEEE Trans. Nucl. Sci. 50 (2003) 998.

[9] E. L. Hull and R. H. Pehl, Nucl. Instr. Meth. A 538 (2005) 651.

[10] P. N. Luke, IEEE Trans. Nucl. Sci. 31 (1984) 312.

[11] D. Protic and G. Riepe, IEEE Trans. Nucl. Sci. 32 (1985) 553.

[12] N. W. Ashcroft and N. D. Mermin, Solid State Physics, Saunders College, Philadelphia, 1976, p. 363.

[13] P. N Luke, M. Amman, J. S. Lee, and J. T. Walton, “Amorphous-Ge and amorphous-Si contacts on Ge detectors,” presented at the IEEE Nuclear Science Symposium in Toronto, Ontario, Canada, 1998.

[14] B. F. Phlips, W. N. Johnson, R. A. Kroeger, et al., IEEE Trans. Nucl. Sci. 49 (2002) 597.

[15] K. P. Ziock, N. Madden, E. Hull, et al., IEEE Trans. Nucl. Sci. 49 (2002) 1737.

[16] S. E. Boggs, W. Coburn, D. M. Smith, et al., New Astr. Rev. 48 (2004) 251.

[17] J. D. Bowen, M. E. Bandstra, S. E. Boggs, et al., Proceedings of the SPIE 6266, (2006) 626625.

Figure captions

Figure 1. Germanium-based gamma-ray detector configurations. (a) Conventional simple planar detector with Li-diffused anode and B-implanted cathode. (b) Position-sensitive detector produced using the conventional contact technologies. (c) Position-sensitive detector produced using the amorphous-semiconductor contact technology.

Figure 2. Measured leakage current plotted as a function of bias voltage at three different temperatures for a p-type Ge detector fabricated with a-Ge electrical contacts (a-Ge/p-type Ge/a-Ge device). The detector thickness and active area were 1 cm and 1.7 cm^2, respectively.

Figure 3. Measured leakage current as a function of bias voltage for Ge detectors at various temperatures. (a) Detector with a configuration of Li diffusion/p-type Ge/a-Ge (Ar + 17.5% H_2). The detector thickness and area were 0.6 cm and 3.5 cm^2, respectively. (b) Detector with a configuration of B implant/n-type Ge/a-Ge (Ar + 17.5% H_2). The detector thickness and area were 0.6 cm and 3.1 cm^2, respectively.

Figure 4. Plot illustrating the barrier height extraction from the data of Figure 3.

Figure 5. Measured leakage current as a function of bias voltage for Ge detectors at various temperatures. (a) Detector with a configuration of a-Ge (Ar + 17.5% H_2)/p-type Ge/a-Ge (Ar + 17.5% H_2). The detector thickness and active area were 1 cm and 1 cm^2, respectively. (b) Detector with a configuration of a-Ge (Ar + 17.5% H_2)/p-type Ge/a-Si (Ar + 7% H_2). The detector thickness and area were 1 cm and 1 cm^2, respectively.

Table caption

Table 1. Extracted barrier heights for amorphous semiconductor contacts on high purity Ge. The sum of the electron and hole barrier heights and film resistivities measured at 77 K are also listed.

Contact	ϕ_e [eV]	ϕ_h [eV]	$\phi_e + \phi_h$ [eV]	ρ [Ω-cm]
a-Ge (Ar)	0.36	0.34	0.70	~ 10^6-10^8
a-Ge (Ar + 17.5% H_2)	0.29	0.39	0.68	~ 10^{11}
a-Si (Ar)	0.39	0.28	0.67	~ 10^9

Table 1.

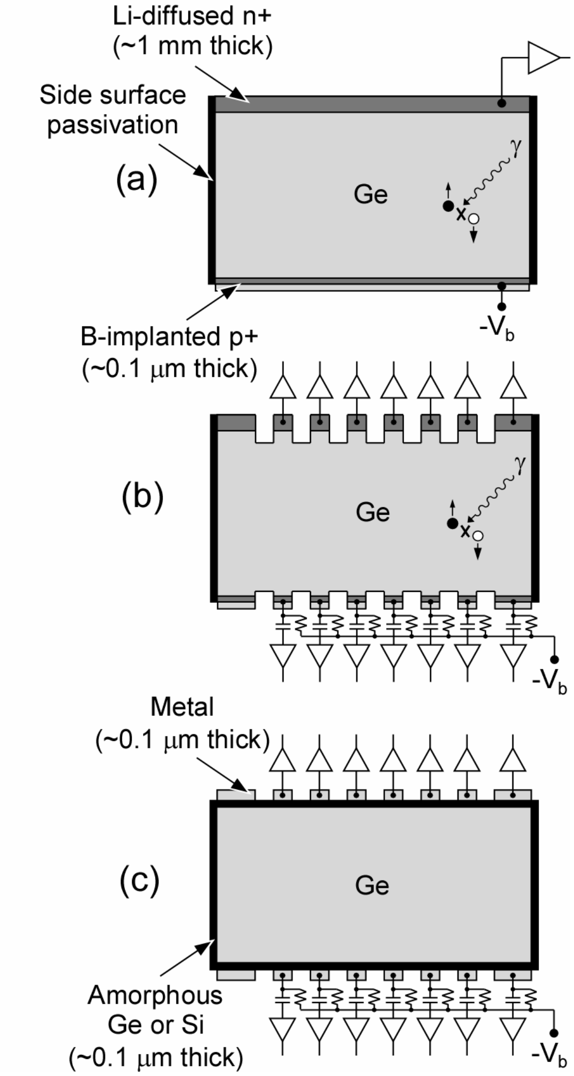
Li-diffused n+
(~1 mm thick)
Side surface
passivation
(a)
Ge
γ
x
B-implanted p+
(~0.1 μm thick)
-V_b
(b)
Ge
γ
x
-V_b
Metal
(~0.1 μm thick)
(c)
Ge
Amorphous
Ge or Si
(~0.1 μm thick)
-V_b

Figure 1.

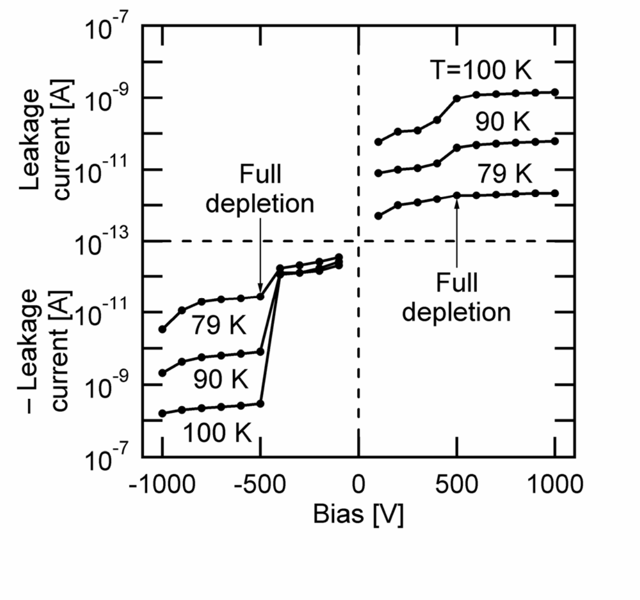

10^{-7}
10^{-9}
10^{-11}
10^{-13}
10^{-11}
10^{-9}
10^{-7}
Leakage current [A]
– Leakage current [A]
T=100 K
90 K
79 K
Full depletion
Full depletion
79 K
90 K
100 K
-1000
-500
0
500
1000
Bias [V]

Figure 2.

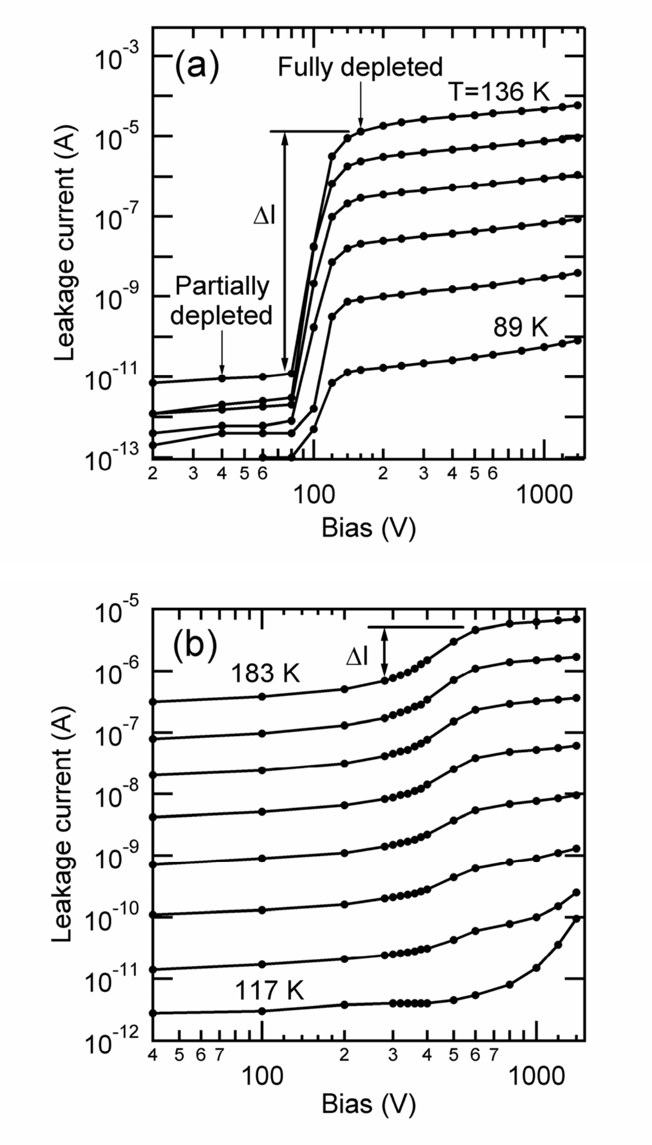
(a)
Fully depleted
T=136 K
ΔI
Partially depleted
89 K
Leakage current (A)
10^-3
10^-5
10^-7
10^-9
10^-11
10^-13
2
3
4
5
6
100
2
3
4
5
6
1000
Bias (V)
(b)
183 K
ΔI
117 K
Leakage current (A)
10^-5
10^-6
10^-7
10^-8
10^-9
10^-10
10^-11
10^-12
4
5
6
7
100
2
3
4
5
6
7
1000
Bias (V)

Figure 3.

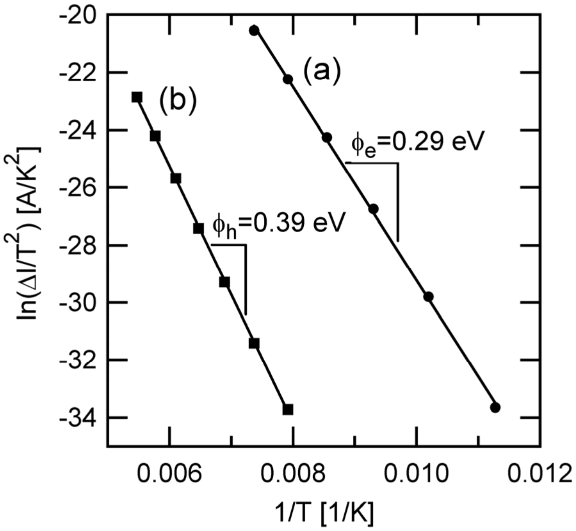

-20
-22
-24
-26
-28
-30
-32
-34
ln(ΔI/T²) [A/K²]
0.006
0.008
0.010
0.012
1/T [1/K]
(a)
(b)
ϕ_e=0.29 eV
ϕ_h=0.39 eV

Figure 4.

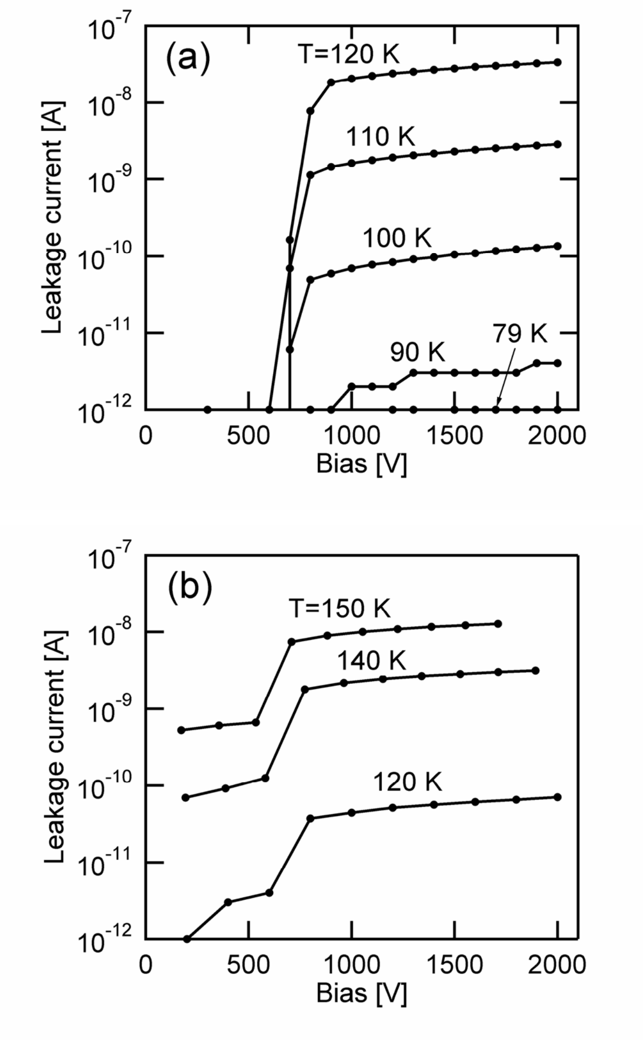
(a)
T=120 K
110 K
100 K
90 K
79 K
Leakage current [A]
10^{-7}
10^{-8}
10^{-9}
10^{-10}
10^{-11}
10^{-12}
0
500
1000
1500
2000
Bias [V]
(b)
T=150 K
140 K
120 K
Leakage current [A]
10^{-7}
10^{-8}
10^{-9}
10^{-10}
10^{-11}
10^{-12}
0
500
1000
1500
2000
Bias [V]

Figure 5.